Myotube Depolarization Generates Reactive Oxygen Species Through NAD(P)H Oxidase; ROS-Elicited Ca^{2+} Stimulates ERK, CREB, Early Genes

ALEJANDRA ESPINOSA,[1] AIDA LEIVA,[2] MARISOL PEÑA,[2] MARIOLLY MÜLLER,[2] ANIBAL DEBANDI,[2] CECILIA HIDALGO,[2] M. ANGÉLICA CARRASCO,[2] AND ENRIQUE JAIMOVICH[2]*

[1]*Escuela de Tecnología Médica, Facultad de Medicina, Universidad de Chile, Santiago, Chile*

[2]*Centro de Estudios Moleculares de la Célula, Instituto de Ciencias Biomédicas, Facultad de Medicina, Universidad de Chile, Santiago, Chile*

Controlled generation of reactive oxygen species (ROS) may contribute to physiological intracellular signaling events. We determined ROS generation in primary cultures of rat skeletal muscle after field stimulation (400 1-ms pulses at a frequency of 45 Hz) or after depolarization with 65 mM K^+ for 1 min. Both protocols induced a long lasting increase in dichlorofluorescein fluorescence used as ROS indicator. Addition of diphenyleneiodonium (DPI), an inhibitor of NAD(P)H oxidase, PEG-catalase, a ROS scavenger, or nifedipine, an inhibitor of the skeletal muscle voltage sensor, significantly reduced this increase. Myotubes contained both the $p47^{phox}$ and $gp91^{phox}$ phagocytic NAD(P)H oxidase subunits, as revealed by immunodetection. To study the effects of ROS, myotubes were exposed to hydrogen peroxide (H_2O_2) at concentrations (100–200 μM) that did not alter cell viability; H_2O_2 induced a transient intracellular Ca^{2+} rise, measured as fluo-3 fluorescence. Minutes after Ca^{2+} signal initiation, an increase in ERK1/2 and CREB phosphorylation and of mRNA for the early genes *c-fos* and *c-jun* was detected. Inhibition of ryanodine receptor (RyR) decreased all effects induced by H_2O_2 and NAD(P)H oxidase inhibitors DPI and apocynin decreased ryanodine-sensitive calcium signals. Activity-dependent ROS generation is likely to be involved in regulation of calcium-controlled intracellular signaling pathways in muscle cells.

Skeletal muscle responds to exercise or electrical stimuli with an increased generation of reactive oxygen species (ROS) (Dröge, 2002; Reid and Durham, 2002). Superoxide anion is released to the extracellular medium in mouse adult muscle during a short period of contractile non-damaging activity; this release originates from myocytes and not from other cell types present within the skeletal muscle tissue in vivo, as shown in myotubes in culture (McArdle et al., 2001). Likewise, both H_2O_2 and nitric oxide (NO), a reactive nitrogen species, are formed in primary skeletal muscle cells during contractions induced by electrical stimulation (Silveira et al., 2003). Superoxide anion can be generated by mitochondrial respiration, xanthine oxidase, uncoupled NO synthase, or via NAD(P)H oxidase (NOX) (Dröge, 2002; Lambeth, 2004). During physical exercise, mitochondria can play a significant role as a source of ROS, since there is a large oxygen flux to mitochondria, and a small fraction of the oxygen may be converted to ROS (Servais et al., 2003). A constitutively active NOX enzyme complex that also contributes to ROS production exists in rat skeletal muscle fibers (Javesghani et al., 2002). These authors detected mRNA and proteins of $p22^{phox}$, $gp91^{phox}$, $p47^{phox}$, and $p67^{phox}$ subunits in skeletal muscle homogenates, which were localized in close proximity to the sarcolemma. The same NOX protein subunits were detected in transverse tubules and triads isolated from rabbit skeletal muscle but not in sarcoplasmic reticulum vesicles (Hidalgo et al., 2006). In addition, skeletal muscle SR contains a DPI-insensitive NADH-dependent oxidase activity that reduces molecular oxygen to generate superoxide (Xia et al., 2003). Superoxide anion is converted to H_2O_2 by superoxide dismutase (SOD) or by spontaneous dismutation (Dröge, 2002), and an increase in SOD activity, among other redox-related enzymes, has been demonstrated in muscle following contractile activity (McArdle et al., 2001; Servais et al., 2003) as well as in skeletal muscle cells exposed to oxidative challenges (Franco et al., 1999; Catani et al., 2004).

In several cell systems, H_2O_2 modifies the function of various proteins including transcription factors, kinases, and phosphatases (Rhee et al., 2000; Dröge, 2002). In smooth muscle cells exposed to H_2O_2, there is an increase of c-fos and c-jun proteins (Rao, 2000) and c-fos mRNA (Ichiki et al., 2003). Activated ERKs and CREB following EGFR transactivation participate in the signaling cascade involved in c-fos mRNA expression in vascular smooth muscle cells (Ichiki et al., 2003). ERKs, and the other MAPKs p38, and JNK, are activated by H_2O_2 in many different cell types (Martindale and Holbrook, 2002; Song et al., 2005). In C2C12 skeletal muscle cells, the increase in AP-1-driven transcription induced by Angiotensin II could be mediated by ROS (Puri et al., 1995). This skeletal cell line responds to exogenous H_2O_2 with activation of the transcription factors NFκB and AP-1, which would be involved in the upregulation of several genes coding for

M. Angélica Carrasco and Enrique Jaimovich have contributed equally to this work.

Contract grant sponsor: Fondo Nacional de Investigación en Areas Prioritarias (FONDAP) Grant; Contract grant number: 15010006.

*Correspondence to: Enrique Jaimovich, ICBM, Facultad de Medicina, Universidad de Chile, Casilla 70005, Santiago 7, Chile. E-mail: ejaimovi@med.uchile.cl

redox-sensitive enzymes (Zhou et al., 2001; Catani et al., 2004).

H_2O_2 can also induce changes in intracellular calcium, which are the result of oxidative modification of calcium channels or other proteins involved in calcium signaling (Dröge, 2002; Waring, 2005). While ROS-induced calcium mobilization has been described in several cell systems (Dröge, 2002), there is no related information in skeletal muscle cells.

We have previously studied depolarization-induced calcium signals in skeletal muscle cells, describing a fast calcium transient involved in excitation-contraction coupling, and a slow nuclear-associated calcium transient unrelated to contraction (Jaimovich et al., 2000; Araya et al., 2003). The slow calcium transient regulates the depolarization-induced activation of ERKs, CREB, and of the early genes *c-fos* and *c-jun* (Powell et al., 2001; Araya et al., 2003; Carrasco et al., 2003; Cardenas et al., 2004). In the present study, we studied ROS production mediated by NAD(P)H oxidase after electrical stimulation and membrane depolarization. We also studied the calcium signals induced by H_2O_2 in skeletal muscle cells in primary culture, as well as the activation of ERKs, CREB, and the early genes *c-fos* and *c-jun* produced by H_2O_2.

Our results indicate that both electrical stimulation and depolarization induced ROS production in skeletal muscle cells, at least partly through NAD(P)H oxidase activation. The H_2O_2-induced calcium transients were mediated primarily by the ryanodine receptor (RyR) calcium release channels. Furthermore, selective RyR inhibition with micromolar ryanodine significantly decreased the activation of ERKs, CREB, and the early genes *c-fos* and *c-jun*, strongly suggesting that these responses are mediated by H_2O_2-induced RyR-mediated calcium release.

MATERIALS AND METHODS

Reagents

DMEM/F-12 was from Sigma Chemical Co. (St. Louis, MO). FCS, calf serum, penicillin/streptomycin 100 U/L, fungizone were from Invitrogen Life Technologies, Inc. (Gaithersburg, MD). Antibodies against dually phosphorylated forms of ERK-1 and ERK-2, against P-CREB and anti-total ERKs were from Cell Signaling Technology (Beverly, MA). CREB antibody and anti-ERK2 were from UBI (Lake Placid, NY). Anti $p47^{phox}$ was from SantaCruz Biotechnology (Cat. # SC7660) and anti $gp91^{phox}$ from BD Biosciences (Cat. # 611414). HRP-conjugated anti-rabbit was from Pierce (Rockford, IL), and HRP-conjugated anti-mouse was from Sigma. Enhanced chemiluminescence reagents were from Pierce or Amersham Pharmacia Biotech (UK). Fluo-3-acetoxymethylester (fluo- 3AM), 5-(and 6)-chloromethyl-2′,7′-dichlorodihydrofluorescein diacetate (CM-H_2DCFA) was from Molecular Probes (Eugene, OR). 2-aminoethoxydiphenyl borate (2-APB) was from Aldrich (St. Louis, MO). All other reagents were purchased from Sigma (St. Louis, MO), Merck (Darmstadt, Germany), or Invitrogen. Assay kit for cell viability was from Molecular Probes (Cat. # L3224).

Cell culture

Rat skeletal muscle cells in primary culture were prepared as previously described (Estrada et al., 2000). Briefly, hind limb muscle from neo-natal Sprague–Dawley rats were mechanically dispersed and treated with 0.2% (w/v) collagenase. The suspension was filtered through optical lens paper (Thomas Scientific), spun down at 200 g for 10 min, and preplated to remove contaminating fibroblasts. Cells were plated on 60-mm culture dishes or on coverslips contained in 35-mm culture dishes for immunostaining procedures. Plating medium was DMEM-F12 (1:1) supplemented with 10% bovine serum, 2.5% FBS, 100 U/L penicillin/streptomycin, 2.5 mg/L fungizone. To eliminate remaining fibroblasts, 10 μM cytosine arabinoside was added after 2 days. To induce differentiation, cells were cultured in DMEM-F12 (1:1) without both bovine serum and FBS for 48–72 h. Experiments were performed in 6 to 7-day-old cultures.

Calcium measurement

Cytosolic calcium images were obtained from single, non-spontaneously contracting myotubes pre-loaded with fluo3-acetoximethylester (fluo-3AM) using an inverted confocal microscope (Carl Zeiss Pascal 5 LSM Microsystems, Jena, Germany) or a fluorescence microscope (Olympus TO41, New Hyde Park, NY) equipped with a cooled CCD camera and image acquisition system (MCD 600, Spectra Source, Westlake Village, CA). Myotubes were washed three times with Krebs buffer (10 mM HEPES-Na, pH 7.4, 145 mM NaCl, 5 mM KCl, 2.6 mM $CaCl_2$, 1 mM $MgCl_2$, 5.6 mM glucose,) and loaded with 5.4 μM fluo-3AM (added from a stock in 20% pluronic acid-DMSO) for 30 min at room temperature. After loading, myotubes were washed with Krebs buffer and used within 2 h. Cell-containing coverslips were mounted in a 1 ml capacity plastic chamber and placed in the microscope for fluorescence measurements after excitation with a 488 nm wavelength argon laser beam or filter system. Cells were stimulated using either H_2O_2 or electrical external electrodes. Fluorescence images were collected and analyzed frame by frame with the image data acquisition program (Spectra-Source) of the equipment. Intracellular calcium was expressed as a percentage of fluorescence intensity relative to basal fluorescence (a value stable for at least 5 min in resting conditions). Digital image processing was performed as described (Estrada et al., 2000).

Western blot analysis

Cells, controls and stimulated, were solubilized at 4°C in 60 μl of lysis buffer containing 50 mM Tris-HCl pH 7.4, 150 mM NaCl, 1 mM EDTA, 1% NP-40, 5 mM Na_3VO_4, 20 mM NaF, and a protease inhibitor cocktail Calbiochem-Novabiochem Corp. (San Diego, CA). The cell lysates were sonicated for 1 min, incubated on ice for 30 min, and centrifuged to remove debris. Proteins were resolved in 10% SDS–polyacrylamide gels and transferred to PDVF membranes. Incubations with primary antibodies were carried out at 4°C overnight using dilutions of 1:1,000 (P-CREB), 1:750 (CREB), 1:2,000 (P-ERKs or total ERKs), 1:500 (gp91), 1:1,000 (p47). After incubation with HRP-conjugated secondary antibodies during 1.5 h, membranes were developed by enhanced chemiluminescence according to the manufacturer's instructions. In order to correct for loading, membranes were stripped and blotted for anti-ERK2, anti-ERKs, and anti-CREB. After scanning the films, a densitometric analysis of the bands was performed with the Scion Image program from NIH.

Immunocytochemistry

Cells placed in coverslips were fixed with methanol at −20°C for 15 min. The blockade was in 1% BSA and the incubation of the primary antibodies was overnight at 4°C. Cells were then washed and incubated with secondary antibody during 1 h at room temperature. Coverslips were mounted in Vectashield (Vector Laboratories, Inc., Burlingame, CA) for confocal microscopy and representative images were acquired (Carl Zeiss Pascal 5, LSM). Negative controls used only secondary antibodies. The images reproduced herein were manipulated in Image J (free software: http://rsb.info.nih.gov/nih-image/Default.html) to improve clarity; no information was added or deleted by those adjustments.

Semi-quantitative RT-PCR

RT was performed as previously reported (Carrasco et al., 2003). cDNA was amplified using c-fos and c-jun primers, and the DNA concentration was normalized to GAPDH expression. PCR amplification was maintained in the exponential phase for each product. The c-fos primers used were 5′-AGGCCGACTCCTTCTCCAGCAT-3′ (sense), 5′-CAGATAGCTGCTCTACTTTGC-3′ (antisense), corresponding to bases 235–533.

The c-jun primers used were 5′-GCGCCGCCGGAGAACCTC TGTC-3′ (sense) and 5′-CAGCTCCGGCGACGCAG CTTG-3′ (antisense).

Determination of ROS production

We determined ROS generation in skeletal muscle cells using CM-H_2DCFA. Myotubes were cultured on glass coverslips and incubated with 5 μM CM-H_2DCFA for 15 min at 37°C. The cells on coverslips were washed with PBS and placed on the camera. Cultures on coverslips dishes were transferred to the confocal microscope (Carl Zeiss Pascal 5, LSM). CM-H_2DCFA fluorescence was detected using excitation at 488 nm and emission at 510–540 nm. In all measurements, a control with laser excitation only was performed. The laser illumination was kept as a minimum (stand by position, 0.1–0.3% potency).

Cell viability

For H_2O_2 toxicity experiments, cells were incubated with cell culture medium without bovine serum and phenol red for 120 min. Cells were visualized in a Nikon Diaphot inverted fluorescence microscope. Toxicity was measured by counting live and dead cells after staining with 0.5 μM Calcein AM and 5 μM ethidium heterodimer-1 (Molecular Probes, cat# L-3224) for 45 min at room temperature. Calcein is a marker for live cells, and ethidium heterodimer-1 intercalates in the DNA of dead cells, giving a green and red fluorescent signal, respectively (Vaughan et al., 1995).

RESULTS

ROS detection in stimulated myotubes

We used the redox sensitive dichlorofluorescein fluorescent probes (CM-H_2DCFA) to record ROS production in myotubes. Figure 1A shows a representative experiment in which the fluorescence of CM-H_2DCFA increased after electrical field stimulation relative to the control. On average, increased ROS production started 2–20 sec after stimulation and a clear difference between control (laser illumination without stimulation) and stimulated cells was always apparent. The difference in fluorescence between control and stimulated cells remained at least for 250 sec. The probe was homogeneously present in the cytoplasm (Fig. 1B). Fluorescence increase was seen as intracellular filament-like structures (arrowhead) and in the nuclear membrane (arrow) 200 sec after electrical stimulation. Comparable fluorescence increase (on average) was obtained when cells were depolarized with high K^+ solutions (Fig. 1A). Addition of 0.5 mM apocynin, an inhibitor of NOX, completely blocked the increase in fluorescence caused by either electrical (Fig. 1C) and K^+-induced depolarization (not shown). Pre-incubation with cell-permeable PEG-catalase produced a similar inhibition. Likewise, 20 μM nifedipine, an inhibitor of the dihydropyridine receptors (DHPRs) skeletal muscle voltage sensor responsible for the activation of membrane potential-dependent calcium release signals, prevented the fluorescence increase produced by depolarization (Fig. 1C).

Presence of NAD(P)H oxidase subunits

To investigate if rat myotubes express NOX subunits, we used polyclonal antibodies against the $p47^{phox}$ cytosolic and $gp91^{phox}$ membrane subunits of the enzyme. Western blot analysis (Fig. 2A) clearly shows bands corresponding to 47 kDa as well as a 58 kDa band present in myotubes extract. Less than 91 KDa molecular weight has been described for the $gp91^{phox}$ subunit in many cell types, including muscle (Javesghani et al., 2002). Upon glycosylation, this protein has been reported to give a 91 KDa band, which appears faintly in our gels (data not shown). As revealed by immunocytochemistry, the $gp91^{phox}$ subunit is present in structures located along the cytosol of the myotubes, which appear sometimes as a longitudinal network (Fig. 2B). The $p47^{phox}$ immunolabel was present mainly in the cytoplasm, albeit distinct label of the plasma membrane was also apparent (Fig. 2C, left part). Thirty seconds

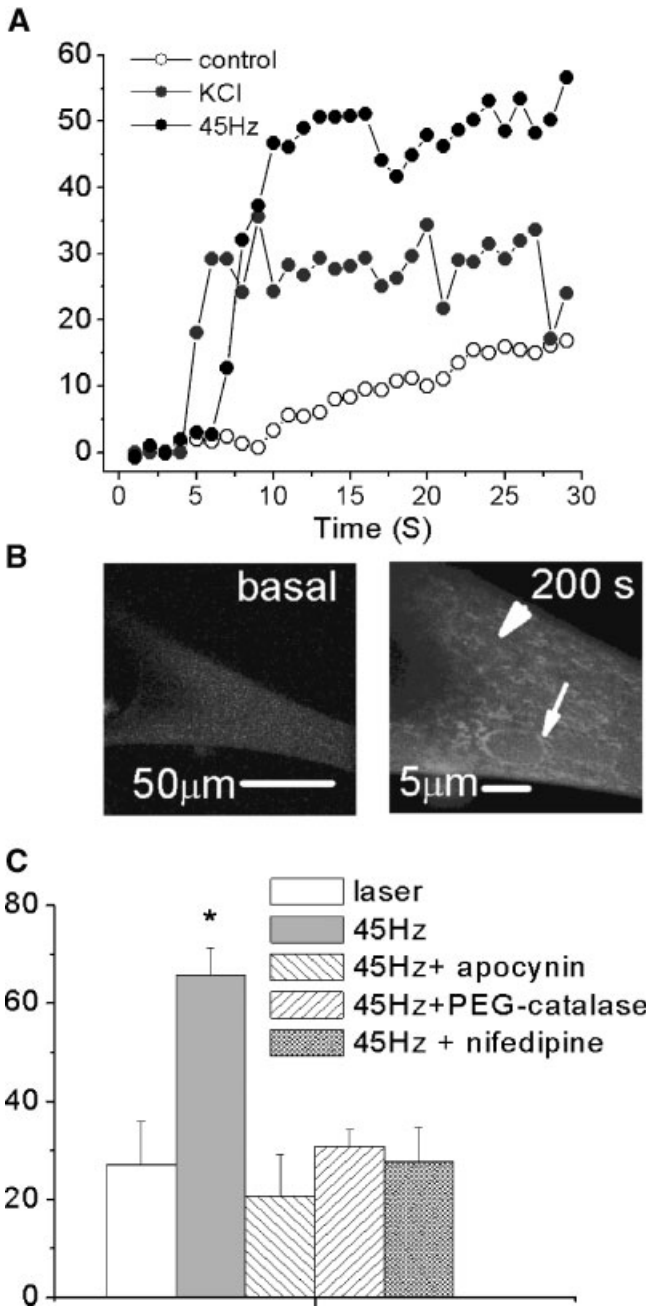

Fig. 1. Electrical stimulation of myotubes produce ROS increase. **A**: The generation of ROS was assayed on the basis of CM-H_2DCFA fluorescence, the figure shows a representative time course of fluorescence increase after both electrical stimulation (400 pulses, 100 msec, 45 Hz), K^+ depolarization and the respective control without stimulation (argon laser). **B**: Fluorescence localization and intensity of the CM-H_2DCFA in the same myotube after loading with the probe (basal) and 200 sec after electrical stimulation. **C**: Fluorescence increase 100 sec after electrical stimulation and the effect of pre-incubation (30 min) with 0.5 mM apocynin (n = 4), 500 U/ml PEG-catalase, and 20 μM nifedipine. Values represent mean ± SEM $^*P < 0.05$, n = 5.

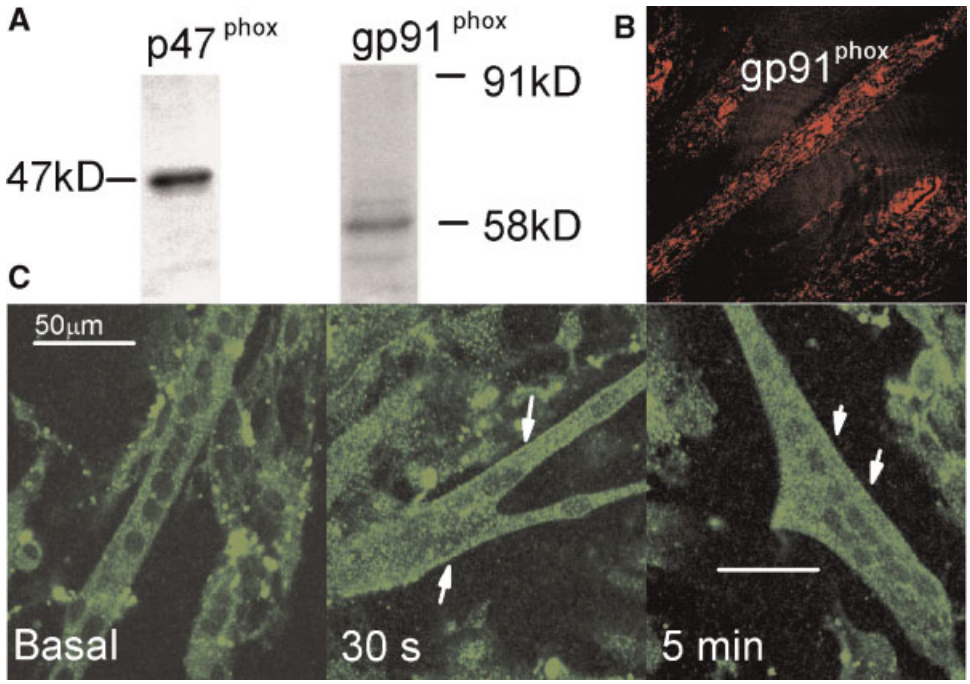

Fig. 2. Immunological detection of $p47^{phox}$ and $gp91^{phox}$ in myotubes. **A**: Western blot analysis of $p47^{phox}$ and $gp91^{phox}$ in whole cell homogenates of cultured myotubes. The first band corresponds to the myotube lysate and consistently co-migrated with a 47kDa molecular marker, the second band with a 58kDa apparent molecular weight corresponds to $gp91^{phox}$. **B**: Immunolocalization of $gp91^{phox}$ using a specific monoclonal antibody, shows distinctive structures longitudinally oriented in the myotube cytosol. **C**: Immunolabeling of $p47^{phox}$ was assessed with polyclonal anti $p47^{phox}$ antibody and fluorescent anti-goat FITC conjugated. Myotubes under basal conditions (left), 30 sec (center) and 5 min (right) during K^+ depolarization were stained. In the latter, a distinct label near the plasma membrane was evident (arrows, center part) and particulate structures were labeled in the cytoplasm, some of them near the plasma membrane appear as striations (arrows right part). Bars represent 20 μm. [Color figure can be viewed in the online issue, which is available at www.interscience.wiley.com.]

after K^+ depolarization, the fluorescent label was more pronounced in the surface membrane area (Fig. 2C, center part). Five min after K^+ depolarization, an apparent translocation of the fluorescent label back to the cytosol took place (Fig. 2C, right part); a striation-like pattern near the borders of the cell was evident (arrows) probably indicating transverse tubular location.

Calcium signals induced by H_2O_2 and electrical stimulation

Addition of H_2O_2 to cultured myotubes induced a transient increase in intracellular calcium concentration; the calcium signal reached a peak at about 150 sec after H_2O_2 addition and lasted for 300 seconds (Fig. 3A). It is important to note that although myotubes were capable of either spontaneous or electrically induced contractions, the cells did neither contract upon H_2O_2 addition nor during the whole experiment. The Ca^{2+} increase took place predominantly in the cell nuclei (Fig. 3E). Noteworthy, H_2O_2-induced Ca^{2+} signals even in the absence of extracellular Ca^{2+} (Fig. 3B), although in these conditions, the signals were in average 30% smaller and longer lasting. Pre-incubation of myocytes with 20 μM ryanodine for 20 min completely prevented the generation of Ca^{2+} signals by H_2O_2 (Fig. 3C). In contrast, addition of H_2O_2 to cells pre-incubated with 50 μM 2-APB (a drug that blocks IP_3-dependent Ca^{2+} signals, Jaimovich et al., 2000) produced Ca^{2+} signals of similar magnitude as the controls, although in this case, the response was considerably delayed by about 30 sec (Fig. 3D). As a control experiment, we tested the viability of myotubes incubated with 50 μM to 10 mM H_2O_2 for 45 min. No cell damage was evident at H_2O_2 concentrations up to 500 μM (data not shown). At 1 mM H_2O_2, some signs of apoptosis (blebbing) were apparent in less than 10% of the cells. In order to evaluate the possible role of NAD(P)H oxidase on ROS production after electrical stimulation of myotubes, field stimulation of myotubes at tetanic frequencies was performed. This procedure produced a large and maintained Ca^{2+} increase (accompanied by cell contraction, not shown) during the whole pulse train indicated by bar (Fig. 3F). In many records, the signal saturated the dye but the mean value of relative fluorescence change for those not saturated was 140 ± 43 ($n = 12$). Addition of either DPI or apocynin significantly decreased the amplitude of the calcium signal (to 64 ± 36, $n = 8$ and 100 ± 13, $n = 6$, respectively) and, in the case of apocynin, oscillations (3–4 in 9 sec) were always apparent indicating that Ca^{2+} release was not enough to maintain a fused tetanus.

Activation of ERKs and CREB by H_2O_2

We have shown previously (Powell et al., 2001; Carrasco et al., 2003) that the generation of IP_3-dependent slow Ca^{2+} signals stimulates ERK and CREB phosphorylation in myotubes. Here, we studied the effects of H_2O_2 on ERK1/2 and CREB activation. Myotubes were stimulated with 200 μM H_2O_2 and the levels of phosphorylated and total ERKs were determined with specific antibodies. Western blots of myotube lysates show significantly increased ERK 2 phosphorylation 10 min after H_2O_2 addition (Fig. 4A). This P-ERK increase was not seen at longer times of exposure to H_2O_2. The H_2O_2-induced increase in ERK1/2 phosphorylation was completely prevented by pre-incubation of cells with 50 μM ryanodine

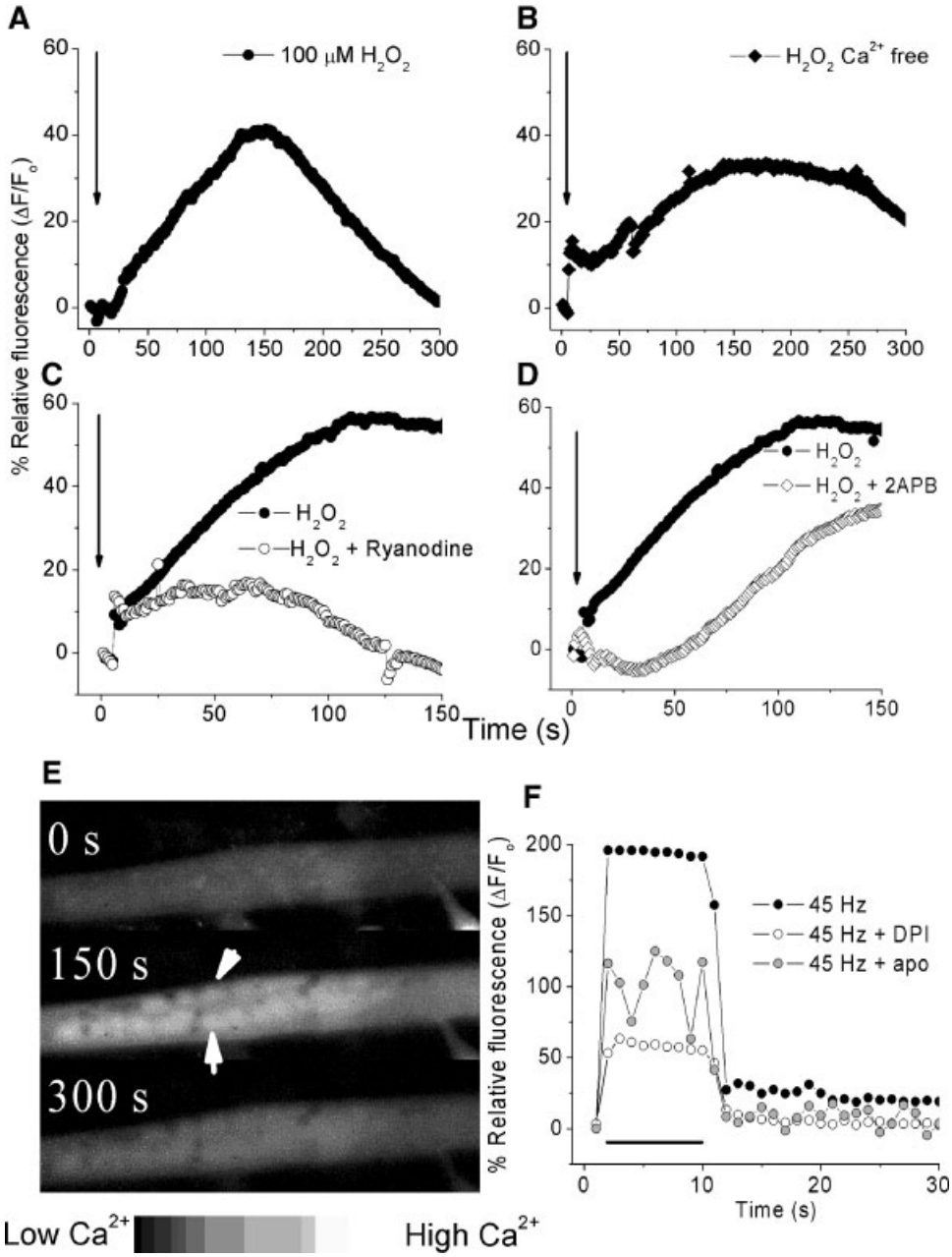

Fig. 3. ROS effects on intracellular calcium signals in myotubes. **A**: Representative kinetics of fluorescence images from a myotube, the sequence shows the peak fluorescence 150 sec after H_2O_2 addition. Intracellular Ca^{2+} is expressed as a percentage of the fluorescence intensity relative to the basal value. **B**: Fluorescence kinetics in calcium free medium (1 mM EGTA); fluorescence was evoked by H_2O_2 and returned to basal values after 300 sec. **C**: In myotubes pre-incubated with 20 μM ryanodine for 20 min, calcium increase induced by H_2O_2 was almost completely inhibited (n = 3). **D**: Effect of pre-incubation of myotubes with 50 μM 2-APB on fluorescence increase produced by H_2O_2 (n = 3). **E**: series of fluo-3 fluorescence images from a myotube taken at indicated times after H_2O_2 (100 μM) addition. **F**: Time course of calcium fluorescence in myotubes during tetanic (400 pulses, 45 Hz) stimulation represented by a horizontal bar. In the control record fluorescence saturates, records in the presence of DPI and apocynin are shown.

(Fig. 4B). Similar results were obtained for CREB phosphorylation. A significant increase in CREB phosphorylation was also evident following 10 min incubation with H_2O_2; CREB phosphorylation reached its maximum at 20 min and decreased after 30 min (Fig. 5A). H_2O_2-induced CREB phosphorylation was completely absent from myotubes pre-incubated with 50 μM ryanodine (Fig. 5B). Total CREB appears increased in Lanes 2, 3, and 4 with respect to Lane 1. This increase was not evident in most experiments. Lane 1 corresponds to control, no H_2O_2, no ryanodine. Extracts from cells exposed to H_2O_2 were loaded in Lanes 2 and 4 only, Lane 3 corresponds to an extract from cells treated with ryanodine as control of cells pre-treated with ryanodine and exposed to H_2O_2 (Lane 4). Therefore, the Western blot suggests increased total CREB both in the presence and in the absence of H_2O_2.

Immunofluorescence studies of P-CREB show fluorescence label increase inside the nuclei (Fig. 5C). In basal conditions, a faint label was present more or less homogeneously in both cytoplasm and nuclei; 15 min after depolarization, the P-CREB label increased

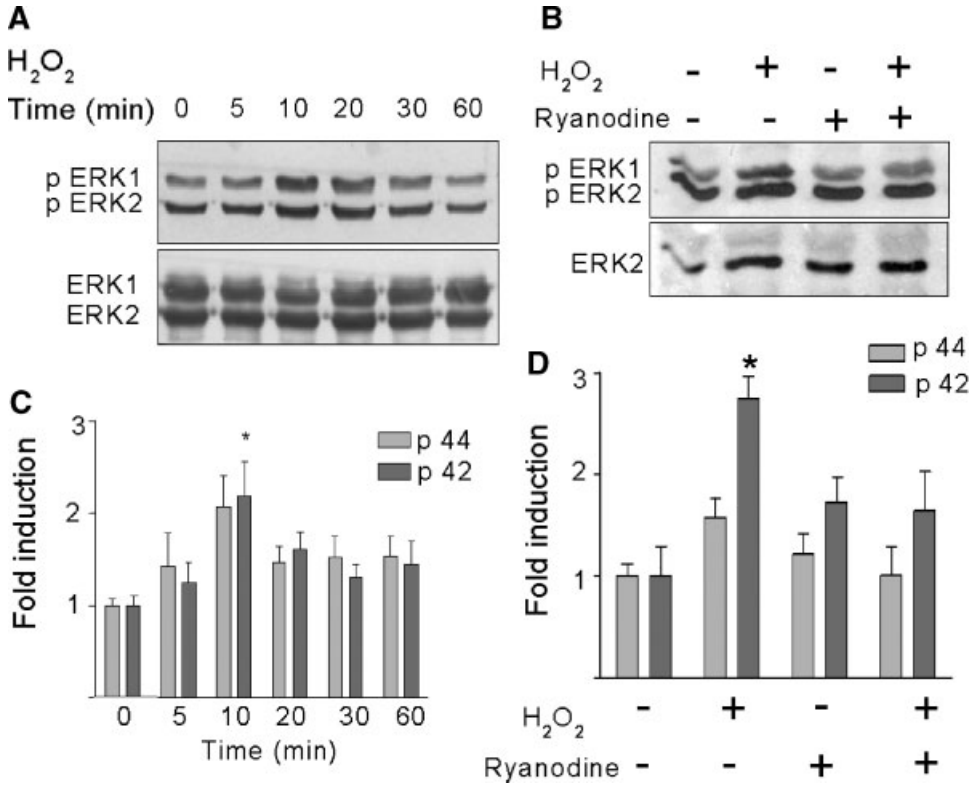

Fig. 4. Effects of hydrogen peroxide on ERK1/2 phosphorylation. **A**: Western blot analysis of P-ERK1/2 or ERK1/2 as loading control, showing the time-dependent effect of 200 μM H_2O_2 on ERK 1/2 phosphorylation. **B**: *Bar graphs* represent P-ERK1 or P-ERK2/total ERKs levels expressed as the average fold increase (mean ± SEM) over basal levels (n = 3–5). There was a significant P-ERK2 increase 10 min after H_2O_2 B addition. **C**: Western blotting for P-ERK1/2 or ERK2 as loading control, in myotubes pre-incubated with or without 50 μM ryanodine for 30 min, and exposed to H_2O_2 for 10 min in the absence or in the presence of ryanodine. **D**: Bar graphs represent P-ERK1 or P-ERK2/ERK2 levels expressed as the average fold increase (mean ± SEM) over basal levels (n = 3) of experiments performed in the absence or in the presence of ryanodine. $^*P < 0.05$.

especially in certain regions of the cytosol. Thirty minutes after stimulus, the label appeared clearly localized in the nuclei. Fluorescence returned to basal levels 60 min after depolarization (Fig. 5C).

Activation of the early genes *c-jun* and *c-fos* by H_2O_2

We have previously reported the depolarization-induced increase of the early genes *c-fos*, *c-jun*, and *egr-1* mRNA levels (Carrasco et al., 2003). This increase is mediated by the IP_3-mediated, slow calcium transient induced by depolarization (Araya et al., 2003; Carrasco et al., 2003). In this work, we have measured mRNA levels of c-fos and c-jun in myotubes exposed to H_2O_2. Expression of mRNA for the immediate early genes *c-fos* and *c-jun* was measured using semiquantitative RT-PCR. After incubation with H_2O_2, mRNA synthesis for both genes increased up to twofold. Significant activation of c-jun and c-fos was already obtained at 15 min of incubation with H_2O_2 (Fig. 6A). Again, the increase in mRNA was prevented by pre-incubation of myotubes with 25 μM ryanodine (Fig. 6B). The results obtained in response to H_2O_2 present the same kinetics and extent of increase than those obtained after depolarization in our model of primary skeletal muscle cells (Carrasco et al., 2003).

DISCUSSION

This work reports two novel observations. The first novel finding is that brief electrical stimulation or short K^+-induced depolarization can elicit ROS generation in skeletal muscle cells in culture. These effects are at least partly mediated by activity dependent stimulation of the NAD(P)H oxidase. The second new observation is that H_2O_2, a mild-oxidant that may possibly act as a physiological second messenger, activates, at non-toxic concentrations, a ryanodine-sensitive calcium-dependent signal transduction cascade involving ERKs, CREB, and immediate early genes.

Receptor-mediated generation of H_2O_2 involving the NOX complex strongly suggests that H_2O_2 should be considered as a signaling messenger (Rhee et al., 2000). The activation of NOX by depolarization has been suggested by results obtained in human and rodent endothelial cells (Sohn et al., 2000; Matsuzaki et al., 2005). In cultured human umbilical vein endothelial cells, changes in membrane potential induced by high K^+ resulted in significant elevation of superoxide formation, whereas hyperpolarization resulted in decrease of superoxide formation (Sohn et al., 2000). The NOX pathway may well be involved since depolarization induced a significant increase in membrane association of the small G protein Rac, a necessary event for activation of some NOX isoforms (Lambeth, 2004). In lung microvascular endothelial cells obtained from rats and mouse, an ischemia-inducing protocol resulted in rapid membrane depolarization and increased ROS generation (Matsuzaki et al., 2005). Moderate to intense electrical stimulation protocols have been reported to induce ROS formation in skeletal muscle (McArdle et al., 2001; Silveira et al., 2003). However in these works,

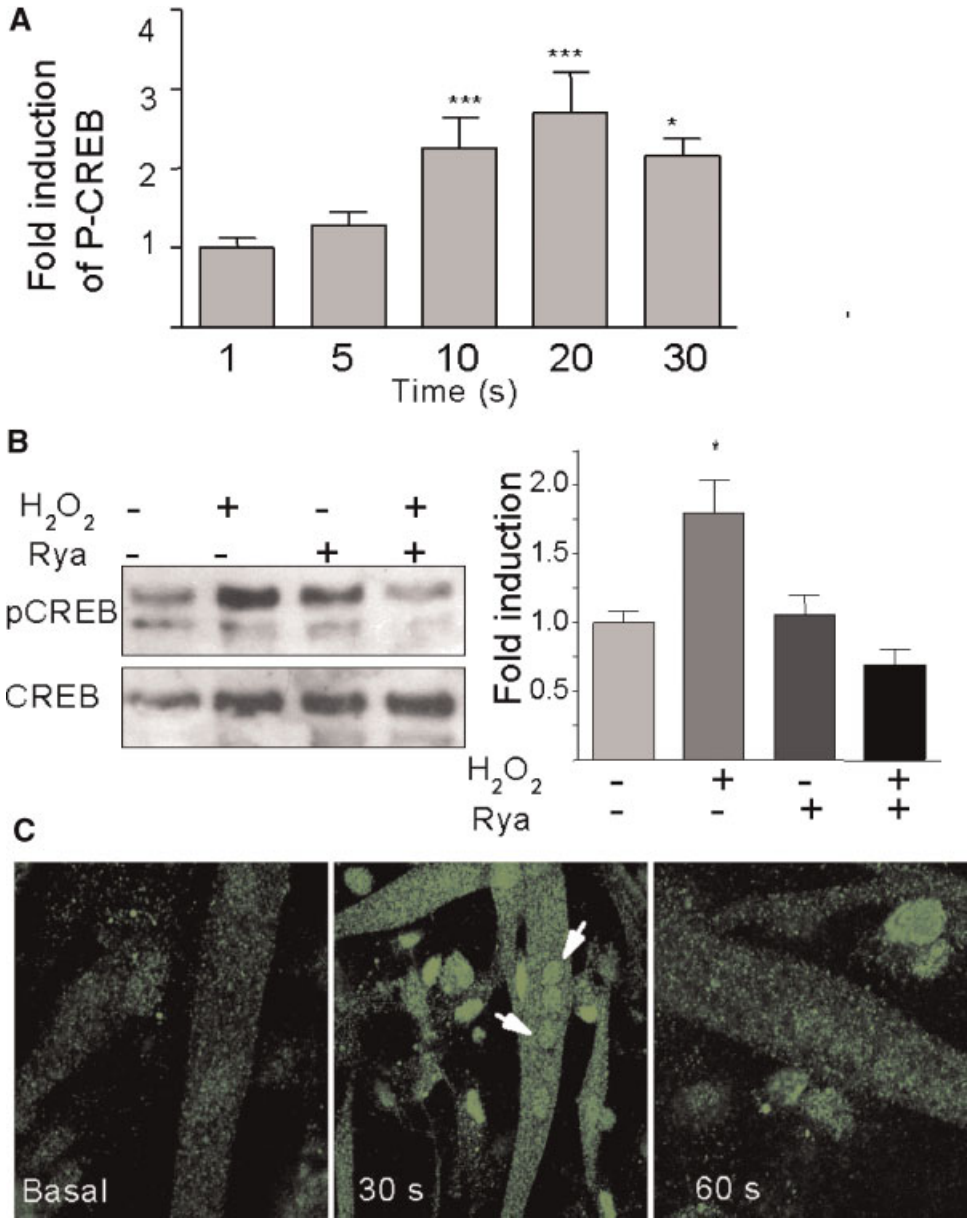

Fig. 5. Hydrogen peroxide induced CREB phosphorylation. **A**: Bar graphs representing P-CREB/total CREB levels expressed as the average fold increase (mean ± SEM) over basal levels, show the increase of CREB phosphorylation at indicated times after H_2O_2 stimulation (n = 3–6). **B**: (left part) Western blotting for P-CREB or total CREB as loading control, in myotubes pre-incubated with or without 50 μM ryanodine for 30 min, and exposed to H_2O_2 for 10 min in the absence or in the presence of ryanodine. Ryanodine produced an almost complete inhibition of CREB phosphorylation (n = 4). (Right part), *bar graphs* represent P-CREB/total CREB levels expressed as the average fold increase (mean ± SEM) over basal levels (n = 4) of experiments performed in the absence or in the presence of ryanodine. *$P < 0.05$; **, $P < 0.001$. **C**: Immunocytochemistry for P-CREB in myotubes; note the difference in location of the label between basal conditions (left part) and 30 sec after stimulation (center parts). Fluorescence returned to basal conditions after 60 sec (right part). [Color figure can be viewed in the online issue, which is available at www.interscience.wiley.com.]

there was no identification of the source of ROS, even though NOX involvement was suggested (McArdle et al., 2001).

We have shown that both high K^+ and electrical stimulation are capable of inducing fast ROS production in cultured muscle cells. The presence of NOX has been detected in both adult muscle fibers (Javesghani et al., 2002) and, recently, in transverse tubule membrane vesicles isolated from skeletal muscle (Hidalgo et al., J. Biol. Chem., in revision). In this work, we show that myotubes also contain this enzyme; our results suggest that this enzyme is fundamentally inactive in resting conditions and the ROS increase is elicited by either membrane depolarization or electrical field stimulation. This increase can be blocked by inhibitors of NOX. Among the inhibitors used, apocynin has been described as a highly specific inhibitor of NOX (Muijsers et al., 2000). Recently, Silveira et al. (2003) demonstrated that both H_2O_2 and NO could be generated during contractions after a protocol of intense electrical stimulation in rat skeletal muscle cells. Possible mechanisms for activation of NOX include Gαi protein interaction and phosphorylation of 47^{phox} subunit by PI3K and PKC (Inoguchi et al., 2003). We have previously reported that voltage activation of DHPRs induces G protein-dependent activation of phospholipase C, possibly via

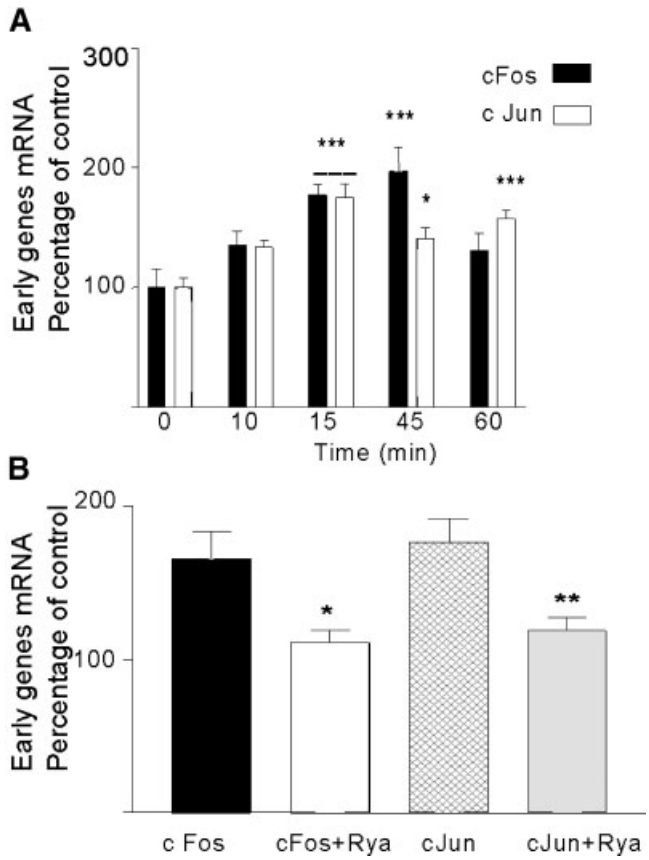

Fig. 6. H_2O_2-induced increase in c-fos and c-jun mRNA levels, is blocked by ryanodine receptor inhibition. **A**: Total RNAs were isolated from myotubes incubated with 200 μM H_2O_2 for the indicated times and mRNA levels were determined by semi-quantitative RT-PCR. The results were normalized to GAPDH expression and presented as percentages of untreated control cells (mean ± SEM) (n = 3–7). $^*P < 0.05$; $^{***}P < 0.0001$, (ANOVA followed by Dunnet's multiple comparison post-test). **B**: Myotubes were pretreated with or without 20 μM ryanodine and exposed to 200 μM H_2O_2. Results obtained at 15 min of exposure to H_2O_2 in the control or experimental series were expressed as percentages of the corresponding control (no H_2O_2). Values are means ± SEM (n = 4–5), $^*P < 0.05$; $^{**}P < 0.001$, compared with the increase obtained in control conditions, H_2O_2 without inhibitor (Student's *t* test for paired data).

activation of Gβγ. This finding probably means that Gαi will be also released upon DHPR activation. Downstream of the Gβγ increase, we have shown PI3K activation (Eltit et al., 2006); this enzyme could in turn activate NOX (Ceolotto et al., 2004). As for PKC activation, we have shown nuclear translocation of PKCα early after membrane depolarization (Cardenas et al., 2004).

Our results point to RyRs as the target for NOX modulation; the calcium signals we see upon H_2O_2 addition have distinct kinetics and significantly differ from those elicited by electrical stimulation (Eltit et al., 2004). The redox state of RyR will change the open probability of the channel (Hidalgo et al., 2004) and thus, is bound to modulate the physiological Ca^{2+} transient in muscle cells. One should expect that if RyRs are modulated by NOX activity, NOX inhibitors should alter RyR-dependent Ca^{2+} signals. Accordingly, both DPI and apocynin were able to modify the Ca^{2+} transient elicited by electrical stimulation of myotubes (Fig. 3F).

ROS can also exert positive or negative modulation on the activity of different calcium channels (Waring, 2005), such as the DHPR (Akaishi et al., 2004) and the RyR (Fill and Copello, 2002; Hidalgo et al., 2005) through oxidative modification of specific protein thiol residues. The RyR1 possesses low affinity inhibitory sites that can be occupied either by Ca^{2+} or Mg^{2+}; noteworthy, RyR1 oxidation or *S*-glutathionylation abolishes the inhibitory effects of Mg^{2+} on calcium-induced calcium release in skeletal muscle (Donoso et al., 2000; Aracena et al., 2003). The RyR has more than 100 cysteine residues per monomer but only a few are highly reactive at physiological pH and are capable of modification by redox agents. Our results support the idea that both signal transduction and H_2O_2-dependent Ca^{2+} signals are part of a process modulated by ROS through RyR oxidation.

To investigate the possible effects of increased ROS generation by conditions that mimic physiological stimulation, we added external H_2O_2 to muscle cells in culture. We have already described that muscle slow calcium transients induce increased ERK1/2 and CREB phosphorylation as well as increased expression of immediate early genes (Powell et al., 2001; Araya et al., 2003; Carrasco et al., 2003; Cardenas et al., 2004). The calcium signals that we have previously studied were triggered by either electrical or hormonal stimulation (Estrada et al., 2000) and were normally dependent on IP_3 production and IP_3 receptors. In this case, calcium release appears to be mainly dependent on redox stimulation of RyRs; the kinetics of the signals is nevertheless slow and more similar to the slow, IP_3-dependent Ca^{2+} transients than to the fast signal related to the excitation–contraction coupling. It is likely then that the magnitude and duration of the signal more than its origin, will determine whether it will be important for contraction or for activating different processes. The contraction-independent slower calcium transients induced by ROS are likely to be involved at the onset of signaling cascades that lead to activation of transcription factors and gene expression, and that are presumably set in motion by enhanced muscle activity (Carrasco et al., 2005). Early genes are activated by slow calcium signals generated by depolarization or by H_2O_2. Upregulation of the expression of the fos and jun gene families after exercise in human skeletal muscle and c-fos and c-jun mRNA increase in rabbit and rat skeletal muscle upon electrical stimulation of the motor nerve (Abu-Shakra et al., 1993; Michel et al., 1994; Aronson et al., 1997) have been reported.

The hypothetical mechanism that couples electrical stimulation to ROS production is depicted in the scheme of Figure 7. DHPRs act as voltage sensors for the electrical stimuli and somehow interact with NOX leading to enhanced ROS production. ROS in turn can activate the RyRs to increase calcium release. In fact, experiments with triad fractions isolated from skeletal muscle revealed that NOX activation enhanced RyR S-glutathionylation and RyR activity (Hidalgo et al., *J. Biol. Chem.*, in revision). This mechanism would proceed in parallel to the known excitation–contraction coupling mechanism in which DHPR directly interacts with RyRs for Ca^{2+} release. Thus, during sustained muscle activation, increased nuclear and cytosolic Ca^{2+} will activate, in addition to contraction, intracellular signaling pathways including ERK and CREB phosphorylation and the transcription of immediate early genes.

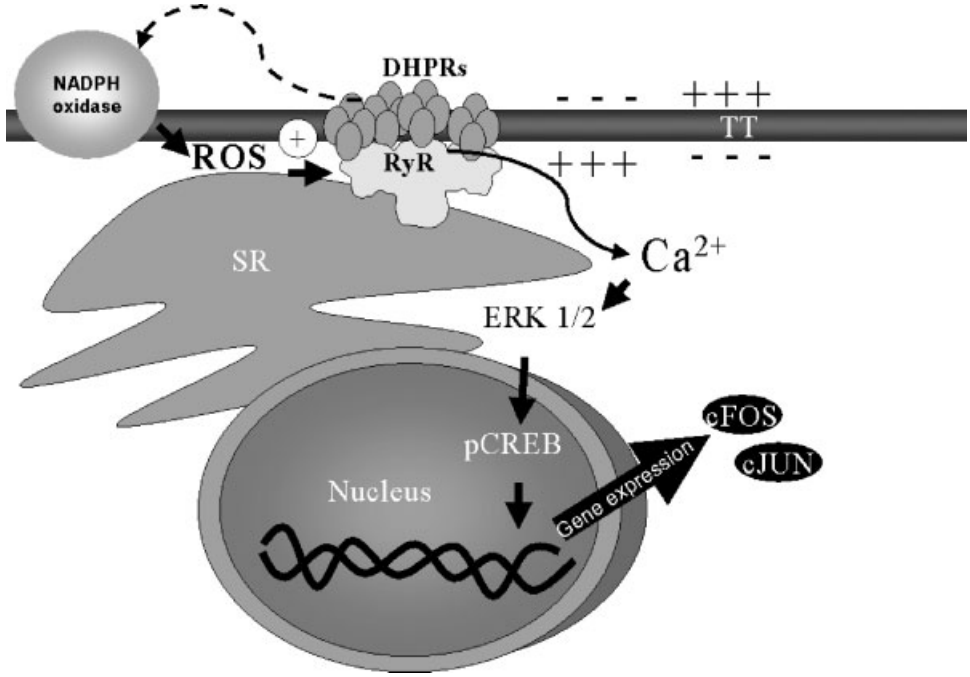

Fig. 7. ROS activate signaling pathways and modulate calcium release. The scheme shows that NADPH oxidase produces ROS after membrane depolarization and activation of DHPRs. A role of ROS on ryanodine receptor open probability is proposed. Probably, ROS induce a positive modulation of calcium release produced by electrical stimulation. Increased calcium induces the activation of ERK 1/2, CREB phosphorylation, and expression of early genes (TT, transverse tubule; SR, sarcoplasmic reticulum).

ACKNOWLEDGMENTS

Authors thank Mónica Silva for cell cultures. This work was supported by Fondo Nacional de Investigación en Areas Prioritarias (FONDAP) Grant 15010006 (to E.J. and C.H.), A.L. and M.P. held student fellowships from the Biophysical Society.

LITERATURE CITED

Abu-Shakra S, Cole AJ, Drachman DB. 1993. Nerve stimulation and denervation induce differential patterns of immediate early gene mRNA expression in skeletal muscle. Mol Brain Res 18:216–220.

Akaishi T, Nakazawa K, Sato K, Saito H, Ohno Y, Ito Y. 2004. Hydrogen peroxide modulates whole cell Ca2+ currents through L-type channels in cultured rat dentate granule cells. Neurosci Lett 356:25–28.

Aracena P, Sanchez G, Donoso P, Hamilton SL, Hidalgo C. 2003. S-glutathionylation decreases Mg2+ inhibition and S-nitrosylation enhances Ca2+ activation of RyR1 channels. J Biol Chem 278:42927–42935.

Araya R, Liberona JL, Cárdenas JC, Riveros N, Estrada M, Powell JA, Carrasco MA, Jaimovich E. 2003. Dihydropyridine receptors as voltage sensors for a depolarization-evoked, IP3R-mediated, slow calcium signal in skeletal muscle cells. J Gen Physiol 121:3–16.

Aronson D, Dufresne SD, Goodyear LJ. 1997. Contractile activity stimulates the c-jun NH_2-terminal kinase pathway in rat skeletal muscle. J Biol Chem 272: 25636–25640.

Cardenas C, Muller M, Jaimovich E, Perez F, Buchuk D, Quest AF, Carrasco MA. 2004. Depolarization of skeletal muscle cells induces phosphorylation of cAMP response element binding protein via calcium and protein kinase Calpha. 279:39122–39131.

Carrasco MA, Riveros N, Ríos J, Müller M, Torres F, Pineda J, Lantadilla S, Jaimovich E. 2003. Depolarization-induced slow calcium transients activate early genes in skeletal muscle cells. Am J Physiol Cell Physiol 284:C1438–C1447.

Catani MV, Savini I, Duranti G, Caporossi D, Ceci R, Sabatini S, Avigliano L. 2004. Nuclear factor kB and activating protein I are involved in differentiation-related resistance to oxidative stress in skeletal muscle cells. Free Rad Biol Med 37:1024–1036.

Ceolotto G, Bevilacqua M, Papparella I, Baritono E, Franco L, Corvaja C, Mazzoni M, Semplicini A, Avogaro A. 2004. Insulin generates free radicals by an NAD(P)H, phosphatidylinositol 3′-kinase-dependent mechanism in human skin fibroblasts ex vivo. Diabetes 53:1344–1351.

Donoso P, Aracena P, Hidalgo C. 2000. Sulfhydryl oxidation overrides Mg(2+) inhibition of calcium-induced calcium release in skeletal muscle triads. Biophys J 79:279–286.

Dröge W. 2002. Free radicals in the physiological control of cell function. Physiol Rev 82:47–95.

Eltit J, Hidalgo J, Liberona JL, Jaimovich E. 2004. Slow calcium signals after tetanic electrical stimulation in skeletal myotubes. Biophys J 86:3042–3051.

Eltit JM, Garcia AA, Hidalgo J, Liberona JL, Chiong M, Lavandero S. 2006. Membrane electrical activity elicits inositol 1,4,5-trisphosphate-dependent slow Ca2+ signals through a Gbetagamma/phosphatidylinositol 3-kinase gamma pathway in skeletal myotubes. J Biol Chem 281:12143–12154.

Estrada M, Liberona JL, Miranda M, Jaimovich E. 2000. Aldosterone- and testosterone-mediated intracellular calcium response in skeletal muscle cell cultures. Am J Physiol Endocrinol Metab 279:E132–E139.

Fill M, Copello JA 2002. Ryanodine receptor calcium release channels. Physiol Rev 82:893–922.

Franco AA, Odom RS, Rando TA 1999. Regulation of antioxidant enzyme gene expression in response to oxidative stress and during differentiation of mouse skeletal muscle. Free Radic Biol Med 27:1122–1132.

Hidalgo C, Bull R, Beherens MI, Donoso P. 2004. Redox regulation of RyR-mediated Ca2+ release in muscle and neurons. Biol Res 37:539–552.

Hidalgo C, Donoso P, Carrasco MA. 2005. The ryanodine receptors Ca^{2+} release channels: Cellular redox sensors? IUBMB Life 57:315–322.

Hidalgo C, Sánchez G, Barrientos G, Aracena-Parks P. 2006. A transverse tubule NOX activity stimulates calcium release from isolated triads via RYR1 S-Glutathionylation. J Biol Chem DOI: 10.1074/jbc.M600451200.

Ichiki T, Tokunou T, Fukuyama K, Iino N, Masuda S, Takeshita A. 2003. Cyclic AMP response element-binding protein mediates reactive oxygen species-induced c-fos expression. Hypertension 42:177–183.

Inoguchi T, Sonta T, Tsubouchi XX, Etoh T, Kakimoto M, Sonoda N, Sato N, Sekiguchi N, Kobayashi K, Sumimoto H, Utsumi H, Nawata H. 2003. Protein kinase C-dependent increase in reactive oxygen species (ROS) production in vascular tissues of diabetes: Role of vascular NAD(P)H oxidase. J Am Soc Nephrol 14:S227–232.

Jaimovich E, Reyes R, Liberona JL, Powell JA. 2000. IP(3) receptors, IP(3) transients, and nucleus-associated Ca(2+) signals in cultured skeletal muscle. Am J Physiol Cell Physiol 278:C998–C1010.

Javesghani D, Magder SA, Barreiro E, Quinn MT, Hussain SN. 2002. Molecular characterization of a superoxide-generating NAD(P)H oxidase in the ventilatory muscles. Am J Respir Crit Care Med 165:412–418.

Lambeth JD 2004. NOX enzymes and the biology of reactive oxygen. Nature Rev Immunol 4:181–189.

Martindale JL, Holbrook NJ. 2002. Cellular response to oxidative stress: Signaling for suicide and survival. J Cell Physiol 192:1–15.

Matsuzaki I, Chatterjee S, DeBolt K, Manevich Y, Zhang Q, Fisher AB. 2005. Membrane depolarization and NADPH oxidase activation in aortic endothelium during ischemia reflect altered mechanotransduction. Am J Physiol Heart Circ Physiol 288:H336–H343.

McArdle C, Pattwell D, Vasilaki A, Griffiths RD, Jackson MT. 2001. Contractile activity-induced oxidative stress: Cellular origin and adaptive responses. Am J Physiol Cell Physiol 280:C621–627.

Michel JB, Ordway GA, Richardson JA, Williams RS. 1994. Biphasic induction of immediate early gene expression accompanies activity-dependent angiogenesis and myofiber remodeling of rabbit skeletal muscle. J Clin Invest 94:277–285.

Muijsers RB, van Den Worm E, Folkerts G, Beukelman CJ, Koster AS, Postma DS, Nijkamp FP. 2000. Apocynin inhibits peroxynitrite formation by murine macrophages. Br J Pharmacol 130:932–936.

Powell J, Carrasco MA, Adams D, Drouet B, Rios J, Múller M, Estrada M, Jaimovich E. 2001. IP_3 receptor fuction and localization in myotubes: An

unexplored Ca^{2+} signaling pathway in skeletal muscle. J Cell Sci 114:3673–3683.
Puri PL, Avantaggiati ML, Burgio VL, Chirillo P, Collepardo D, Natoli G, Balsano C, Levero M. 1995. Reactive oxygen intermediates mediate angiotensin II-induced c-jun-c-fos heterodimer DNA binding activity and proliferative hypertrophic responses in myogenic cells. J Biol Chem 270:22129–22134.
Rao GN. 2000. Oxidant stress stimulates phosphorylation of eIF4E without an effect on global protein synthesis in smooth muscle cells. Lack of evidence for a role of H202 in angiotensin II-induced hypertrophy. J Biol Chem 275:16993–16999.
Reid MB, Durham WJ 2002. Generation of reactive oxygen and nitrogen species in contracting skeletal muscle: Potential impact on aging. Ann NY Acad Sci 959:108–116.
Rhee SG, Bae YS, Lee SR, Kwon J. 2000. Hydrogen peroxide: A key messenger that modulates protein phosphorylation through cysteine oxidation. Science's STKE 53:pe1.
Servais S, Couturier K, Koubi H, Rouanet JL, Desplanches D, Sornay-Mayet MH, Sempore B, Lavoie JM, Favier R. 2003. Effect of voluntary exercise on H_2O_2 release by subsarcolemmal and intermyofibrillar mitochondria. Free Radic Biol Med 35:24–32.
Silveira LR, Pereira-Da-Silva L, Juel C, Hellsten Y. 2003. Formation of hydrogen peroxide and nitric oxide in rat skeletal muscle cells during contractions. Free Rad Biol Med 35:455–464.
Sohn HY, Keller M, Gloe T, Morawietz H, Rueckschloss U, Pohl U. 2000. The small G-protein Rac mediates depolarization-induced superoxide formation in human endothelial cells. J Biol Chem 275:18745–18750.
Song HJ, Lee TS, Jeong JH, Shin CY, Sohn UD. 2005. Hydrogen peroxide-induced extracellular signal-regulated kinase activation in cultured feline ileal smooth muscle cells. J Pharmacol Exp Therapeutics 312:391–398.
Vaughan PJ, Pike CJ, Cotman CW, Cunningham DD. 1995. Thrombin receptor activation protects neurons and astrocytes from cell death produced by environmental insults. J Neurosci 15:5389–5401.
Waring P. 2005. Redox active calcium ion channels and cell death. Arch Biochem Biophys 434:33–42.
Xia R, Webb JA, Gnall LLM, Cutler K, Abramson JJ. 2003. Skeletal muscle sarcoplasmic reticulum contains a NADH-dependent oxidase that generates superoxide. Am J Physiol Cell Physiol 285:C215–C221.
Zhou LZ, Johnson AP, Rando TA. 2001. NF kappa B and AP-1 mediate transcriptional responses to oxidative stress in skeletal muscle cells. Free Radic Biol Med 31:1405–1416.